

# Global quantification of mammalian gene expression control

Björn Schwanhäusser<sup>1</sup>, Dorothea Busse<sup>1</sup>, Na Li<sup>1</sup>, Gunnar Dittmar<sup>1</sup>, Johannes Schuchhardt<sup>2</sup>, Jana Wolf<sup>1</sup>, Wei Chen<sup>1</sup> & Matthias Selbach<sup>1</sup>

**Gene expression is a multistep process that involves the transcription, translation and turnover of messenger RNAs and proteins. Although it is one of the most fundamental processes of life, the entire cascade has never been quantified on a genome-wide scale. Here we simultaneously measured absolute mRNA and protein abundance and turnover by parallel metabolic pulse labelling for more than 5,000 genes in mammalian cells. Whereas mRNA and protein levels correlated better than previously thought, corresponding half-lives showed no correlation. Using a quantitative model we have obtained the first genome-scale prediction of synthesis rates of mRNAs and proteins. We find that the cellular abundance of proteins is predominantly controlled at the level of translation. Genes with similar combinations of mRNA and protein stability shared functional properties, indicating that half-lives evolved under energetic and dynamic constraints. Quantitative information about all stages of gene expression provides a rich resource and helps to provide a greater understanding of the underlying design principles.**

The four fundamental cellular processes involved in gene expression are transcription, mRNA degradation, translation and protein degradation. It is now clear that each step of this cascade is controlled by gene-regulatory events<sup>1,2</sup>. Although each individual process has been intensively studied, little is known about how the combined effect of all regulatory events shapes gene expression. The fundamental question of how genomic information is processed at different levels to obtain a specific cellular proteome has therefore remained unanswered.

With regard to a quantitative description of gene expression, numerous previous studies comparing mRNA and protein levels concluded that the correlation is poor<sup>3,4</sup>. However, the available data suffer from several limitations. Most studies are limited to a few hundred genes, mainly due to the technical challenges involved in large-scale protein identification and quantification. Also, protein levels measured in one experiment are typically compared to mRNA levels determined in a different experiment performed at a different time in a different laboratory, making it difficult to interpret why the correlation is low. Finally, mRNA and protein levels result from coupled processes of synthesis and degradation. Therefore, analysis of mRNA and protein levels alone cannot provide sufficient information to understand gene expression comprehensively. mRNA and protein turnover can be measured with drugs to inhibit transcription or translation<sup>5,6</sup>, but this has severe side effects. Studies based on artificial fusion proteins are problematic because tagging can affect protein stability<sup>7</sup>.

To overcome these limitations we sought to quantify cellular mRNA and protein expression levels and turnover in parallel in a population of unperturbed mammalian cells. Pulse labelling with radioactive nucleosides or amino acids is regarded as the gold standard method to determine mRNA and protein half-lives. Recently, variants of this approach based on non-radioactive tracers have been established<sup>8–10</sup>. In stable isotope labelling by amino acids in cell culture (SILAC), cells are cultivated in a medium containing heavy stable-isotope versions of essential amino acids<sup>11</sup>. When non-labelled (that is, light) cells are transferred to heavy SILAC growth medium, newly synthesized proteins incorporate the heavy label while pre-existing proteins remain in the

light form. This strategy can be used to measure protein turnover<sup>12–14</sup> or relative changes in protein translation<sup>15,16</sup>. Similarly, newly synthesized RNA can be labelled with the nucleoside analogue 4-thiouridine (4sU). 4sU-containing mRNA can be purified and compared with the pre-existing fraction to compute mRNA half-lives<sup>10</sup>.

## Pulse labelling of proteins and mRNAs

We used parallel metabolic pulse labelling with amino acids and 4sU to measure simultaneously protein and mRNA turnover in a population of exponentially growing non-synchronized NIH3T3 mouse fibroblasts (Fig. 1a). Protein samples were collected at three time points, measured by liquid chromatography and online tandem mass spectrometry (LC-MS/MS) and analysed with the MaxQuant software package<sup>17</sup>. We identified 84,676 peptide sequences and assigned them to 6,445 unique proteins (false discovery rate <1% at the peptide and protein level). A total of 5,279 of these proteins was quantified by at least three heavy to light (H/L) peptide ratios (Fig. 1b). Tissue-specific amino acid precursor pools and recycling rates, a pervasive problem for *in vivo* pulse labelling experiments<sup>9,18,19</sup>, did not appreciably affect our results (Supplementary Fig. 1). For constant incorporation rates the logarithm of H/L ratios should increase linearly with time (Fig. 1c). Ninety-three per cent of proteins showed excellent linear correlation indicated by a variability of the linear regression slope smaller than 1% (Fig. 1d). Protein abundance did not influence H/L ratio measurements (Supplementary Fig. 2). In total, we obtained a confident set of 5,028 protein half-lives calculated from the slope of the regression line. Cycloheximide chase experiments for selected proteins spanning a representative range of half-lives agreed well with half-lives determined by pulsed labelling and mass spectrometry (Supplementary Fig. 3). In parallel, we pulse labelled newly synthesized RNA for 2 h with 4sU. RNA samples were fractionated into the newly synthesized and pre-existing fractions. Both fractions and the total RNA sample were analysed by mRNA sequencing and quantified by mapping reads to their exonic region<sup>20</sup>. We calculated mRNA half-lives based on the ratios of newly synthesized RNA/total RNA ratio and the pre-existing RNA/total RNA<sup>10</sup>.

<sup>1</sup>Max Delbrück Center for Molecular Medicine, Robert-Rössle-Str. 10, D-13092 Berlin, Germany. <sup>2</sup>MicroDiscovery GmbH, Marienburger Str. 1, D-10405 Berlin, Germany.

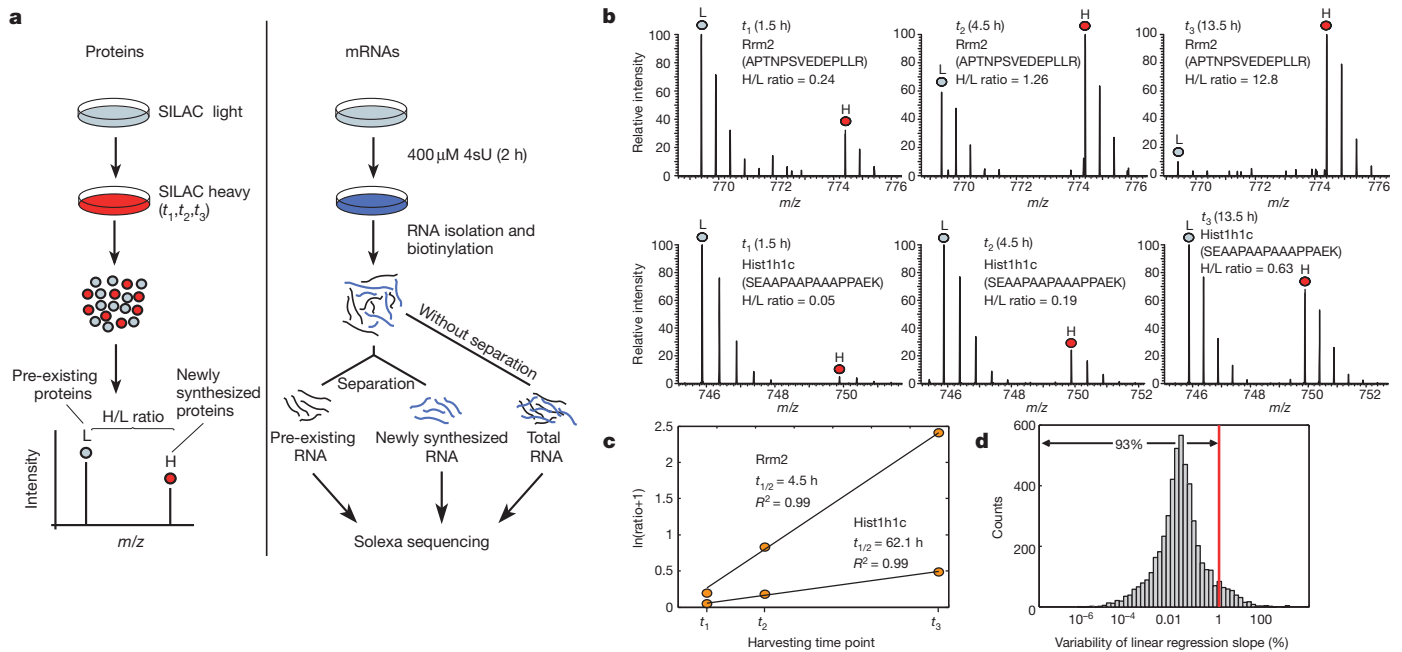


**Figure 1 | Parallel quantification of mRNA and protein turnover and levels.** **a**, Mouse fibroblasts were pulse labeled with heavy amino acids (SILAC, left) and the nucleoside 4-thiouridine (4sU, right). Protein and mRNA turnover was quantified by mass spectrometry and next-generation sequencing, respectively. **b**, Mass spectra of peptides from a high- and low-turnover protein reveal

Proteins were, on average, five times more stable (median half-life of 46 h) than mRNAs (9 h) and spanned a bigger dynamic range (Fig. 2a). Because very long ( $>200$  h) and very short ( $<30$  min) protein half-lives cannot be accurately quantified from our three time points, the true dynamic range of protein stabilities may be even higher. Notably, we found no correlation between protein and mRNA half-lives (Fig. 2c,  $R^2 = 0.02$ , log-log scale).

### Absolute mRNA and protein copy numbers

We calculated absolute cellular mRNA copy numbers based on the number of sequencing reads in the unfractionated sample in conjunction

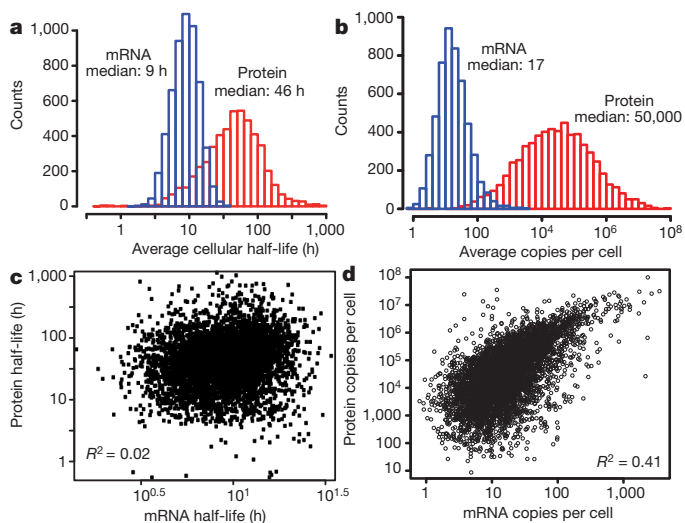


**Figure 2 | mRNA and protein levels and half-lives.** **a**, **b**, Histograms of mRNA (blue) and protein (red) half-lives (**a**) and levels (**b**). Proteins were on average 5 times more stable and 2,800 times more abundant than mRNAs and spanned a higher dynamic range. **c**, **d**, Although mRNA and protein levels correlated significantly, correlation of half-lives was virtually absent.

increasing heavy to light (H/L) ratios over time. **c**, Protein half-lives were calculated from log H/L ratios at all three time points using linear regression. **d**, Variability of linear regression slopes assessed by leave-one-out cross-validation was small.

with information on cellular mRNA content<sup>20</sup>. Absolute protein copy numbers can be inferred from mass spectrometry data<sup>21,22</sup>. To this end, we used the sum of peak intensities of all peptides matching to a specific protein. When divided by the number of theoretically observable peptides, this value provides an accurate proxy for protein levels ('intensity-based absolute quantification' or iBAQ, see Supplementary Methods).

Levels of detected proteins spanned more than five orders of magnitude (Fig. 2b). Relatively few proteins had less than 100 copies per cell, indicating that some proteins of low abundance escaped detection. Indeed, we observed a moderate detection bias (Supplementary Fig. 4) and therefore restricted our analysis to genes that were identified at both the mRNA and protein level. In this subset, proteins were, on average, about 2,800 times more abundant than corresponding transcripts. Despite a huge spread, mRNA and protein levels were clearly correlated (Fig. 2d,  $R^2 = 0.41$ , log-log scale). This correlation is considerably higher than in any previous study in mammals<sup>3,4,23</sup>. An attempt to improve this correlation further by nonlinear transformation resulted only in a marginal increase ( $R^2 = 0.44$ , Supplementary Fig. 5). It seems that for our data set, this is about the maximum correlation between mRNA and protein that can be achieved without additional information.

### Reproducibility

To investigate the experimental noise we performed a second independent large-scale experiment and measured mRNA and protein levels and half-lives again. The overall correlation of half-lives and levels between both replicates was good (Supplementary Fig. 6 and Supplementary Table 1). Removing less-consistent data points did not increase correlation between mRNA and protein levels or half-lives (Supplementary Fig. 7). Thus, noise has little impact on the observed correlation between mRNA and protein levels and half-lives. We also validated absolute mRNA and protein copy numbers using independent methods. For mRNA copy numbers we used the NanoString technology, which captures and counts individual transcripts without enzymatic reactions<sup>24</sup>. Correlation between sequencing and NanoString data was high ( $r = 0.79$ , see also Supplementary Fig. 8a). Absolute protein quantification was validated by spike-in

experiments using a mixture of 48 proteins with known concentrations (Supplementary Fig. 8b). iBAQ values correlated well with known absolute protein amounts over at least four orders of magnitude and had a higher precision and accuracy than alternative measures of absolute protein abundance (data not shown)<sup>21,22</sup>. We also assessed degradation and synthesis rates for mRNAs and proteins by actinomycin D and cycloheximide treatment, respectively. For high turnover proteins and mRNAs we obtained results consistent with pulse labelling data (Supplementary Fig. 8c–f).

### A quantitative model of gene expression

Our data allow us to calculate average synthesis rates of mRNAs and proteins for thousands of genes using a mathematical model (Fig. 3a and Supplementary Methods). The experimental data are based on a population of non-synchronized cells. Therefore, our estimated rates provide an average over the population and time.

Average cellular transcription rates predicted by the model spanned two orders of magnitude with a median of about two mRNA molecules per hour (Fig. 3b). An extreme example was *Mdm2* with more than 500 mRNAs per hour. A microscopic study on the cytomegalovirus (CMV) promoter reported transcription termination rates of 5.8 to 8.7 mRNAs per hour<sup>25</sup>. These values are above the median of our predictions, as perhaps expected for a strong promoter system. Next, we calculated translation rate constants; that is, how many proteins are made from each mRNA template per hour (Fig. 3c). We find a median translation rate constant of about 140 proteins per mRNA per hour. Several proteins involved in translational regulation—such as the translation initiation factor eIF4G1, fragile X syndrome related protein Fxr2 and tuberlin—had extremely low rate constants and were translationally repressed. Plotting translation rate constants against protein levels revealed that abundant proteins are translated at least 100 times more efficiently than those of low abundance (Fig. 3d). Hence, different translation efficiencies contribute to the higher dynamic range of proteins compared to mRNAs (Fig. 2b). Intriguingly, translation rate constants saturated at around 1,000 protein copies per mRNA per hour. To our

knowledge, the maximal translation rate constant in mammals is not known. On the basis of ref. 1, the estimated maximal translation rate constant in sea urchin embryos is 140 copies per mRNA per hour, which is lower than the prediction of our model.

### Control of gene expression

A long-standing question is how much protein abundance is controlled at the transcriptional, post-transcriptional, translational and post-translational levels. Until now, this has mainly been addressed indirectly by analysing mRNA and protein sequence features. Features related to translation initiation (for example, Shine–Dalgarno, Kozak and 3′ untranslated region (UTR) sequences), elongation (for example, codon bias) and protein stability (for example, degrons) have been analysed and reported to correlate partially with protein/mRNA ratios in bacteria, yeast and mammals<sup>23,26,27</sup>. We also observed sequence features characteristic of mRNA and protein stability and found that mRNAs with long 3′ UTRs are, on average, less stable (Supplementary Fig. 9). In addition, the density of AU-rich elements and binding motifs of a specific RNA-binding protein (pumilio 2) correlated negatively with mRNA stability (Supplementary Fig. 10). Highly structured proteins were more stable than unstructured ones (Supplementary Fig. 11a). We also identified amino acids over-represented in unstable proteins (Supplementary Fig. 11b).

Sequence features are at best indirect proxies for mechanisms controlling protein abundance. How much efficiencies of different steps in the gene expression cascade contribute to variance of cellular protein copy numbers can only be revealed by direct parallel genome-scale measurements of mRNA and protein levels and half-lives which were not available previously. In our data the coefficient of determination ( $R^2$ ) between mRNA and protein copy numbers is 0.41 (Fig. 2d). Assuming the absence of technical and biological noise, this means that ~40% of the variance in protein levels is explained by mRNA levels—considerably more than previously thought (Fig. 4a). Most of this 40% is due to different transcription rates, whereas mRNA stability has a smaller role. Considering translation rate constants markedly boosts  $R^2$  to 0.95. Thus, translation rate constants have the dominant role for control of protein levels. Unexpectedly, the impact of protein degradation is rather small.

In the above analysis the same experimental data were used to calculate synthesis rates and to estimate their impact on protein levels. To avoid this over-fit and to assess reliability of the model predictions we performed the same analysis with data from the biological replicate experiment. In the replicate the coefficient of determination between mRNA and protein levels was 0.37 (Fig. 4b). We then used the model including the estimated parameters from the first experiment to predict protein levels from mRNA levels in the replicate data. Predicted protein levels agreed very well with measured protein levels ( $R^2 = 0.85$ , Fig. 4c). Therefore, the model explains ~85% of the variability in protein copy numbers in an independent experiment. The correlation is very similar to the direct comparison of protein levels in both experiments ( $R^2 = 0.84$ , Supplementary Fig. 6d). We conclude that technical and biological noise in our data are low, and that the model faithfully predicts protein levels from mRNA levels in mouse fibroblasts. It also indicates that the estimated impact of transcription, mRNA stability, translation and protein stability on protein abundance is reproducible. We finally assessed how much of the efficiencies of the various steps in gene expression are retained in a different cell type and organism. To this end, we quantified mRNA and protein abundance in the human breast cancer cell line MCF7 by RNA-seq and mass spectrometry, respectively. A total of 2,030 human genes from the MCF7 data set had orthologues in the mouse fibroblast data. We then used rates from the mouse fibroblast model to predict protein levels from mRNA levels in human breast cancer cells. In MCF7 cells, the model predicted ~60% of the variability in protein levels (Fig. 4a). Although the fraction explained by the model is smaller than in mouse fibroblasts, this indicates that translation and degradation rates are to

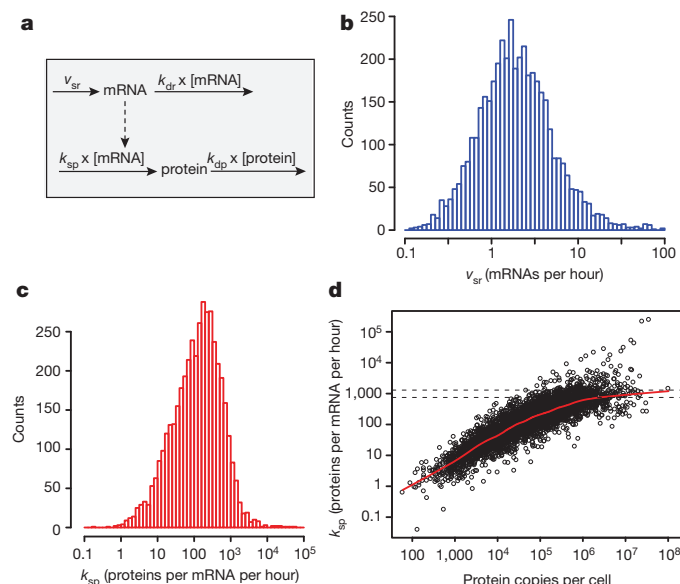


**Figure 3 | Quantitative model of gene expression in growing cells.**

**a**, mRNAs are synthesized with the rate  $v_{sr}$  and degraded with a rate constant  $k_{dr}$ . Proteins are translated and degraded with rate constants  $k_{sp}$  and  $k_{dp}$ , respectively. **b**, Calculated mRNA transcription rates show a uniform distribution. **c**, Calculated translation rate constants are not uniform. **d**, Translation rate constants of abundant proteins saturate between approximately 750 and 1,300 proteins per mRNA per hour. Red line shows the locally weighted fit (Lowess). Dashed lines indicate 95% confidence intervals of the Lowess maximum value calculated by bootstrapping.



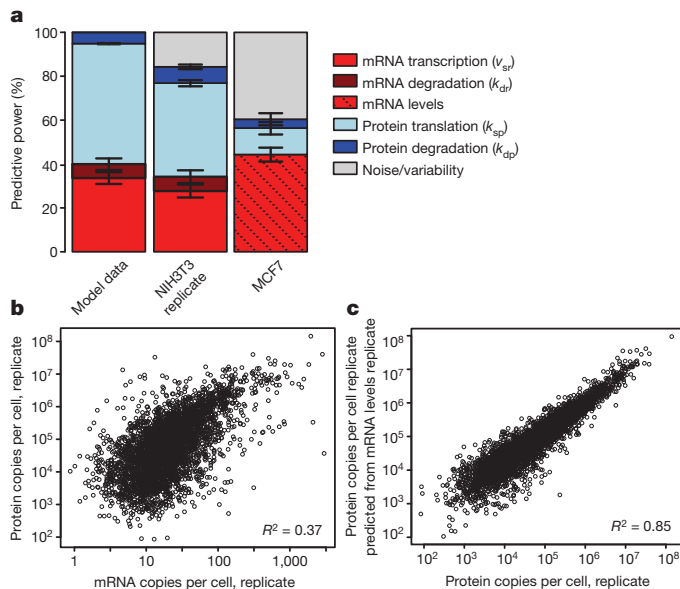


**Figure 4 | Impact of different rates and rate constants on protein abundance.** **a**, Protein levels are best explained by translation rates, followed by transcription rates. mRNA and protein stability is less important (left bar). **b**, In the replicate experiment mRNA levels explained 37% of protein levels in NIH3T3 cells (middle bar in **a**). **c**, The model explains 85% of variance in protein levels from measured mRNA levels (middle bar in **a**). The mouse fibroblast model has some predictive power for human orthologous genes in MCF7 cells (right bar in **a**). Error bars show 95% confidence intervals estimated by bootstrapping.

some extent independent of the cell type and conserved between mouse and human. It is noticeable, however, that the drop in prediction is mainly due to the fact that the translation part of the model performs less well.

### Half-lives and gene function

Degradation of proteins is critically involved in many cellular processes including cell-cycle progression, signal transduction and apoptosis<sup>28–30</sup>. Similarly, mRNA stability is important for the temporal order of gene induction<sup>10,31</sup>. Genes may have evolved specific combinations of mRNA and protein half-lives under functional constraints<sup>10,31,32</sup>. We therefore asked if genes with specific combinations of mRNA and protein stability have distinct biological functions. We grouped genes according to their half-lives and used gene ontology to find enriched biological processes (Fig. 5; see Supplementary Table 2 for a complete list).

Genes with stable mRNAs and stable proteins were enriched in constitutive cellular processes like translation (that is, ribosomal proteins), respiration and central metabolism (glycolysis, citric acid cycle). Hence, many housekeeping genes tend to have stable mRNAs and proteins. In yeast energy costs keep transcription and translation rates under selective pressure<sup>33</sup>. We reasoned that energy constraints may explain why housekeeping genes tend to have stable mRNAs and proteins. On the basis of the model, we calculated the theoretical energy required to maintain cellular mRNA and protein levels by recycling from their building blocks (nucleotide monophosphates and amino acids, respectively) in terms of high energy phosphates. This is a conservative estimate as splicing, folding and transport are not included. Protein synthesis consumes more than 90% of the energy whereas less than 10% is needed for transcription. A total of 20% of the proteins consumed 80% of the energy for translation (Pareto principle or 80/20 rule). Consistent with optimization under energy constraints, abundant proteins were significantly more stable than less abundant ones (Supplementary Fig. 12a,  $P < 10^{-15}$ , Wilcoxon test). This is not necessarily expected because the overall contribution of protein stability to protein levels is very small

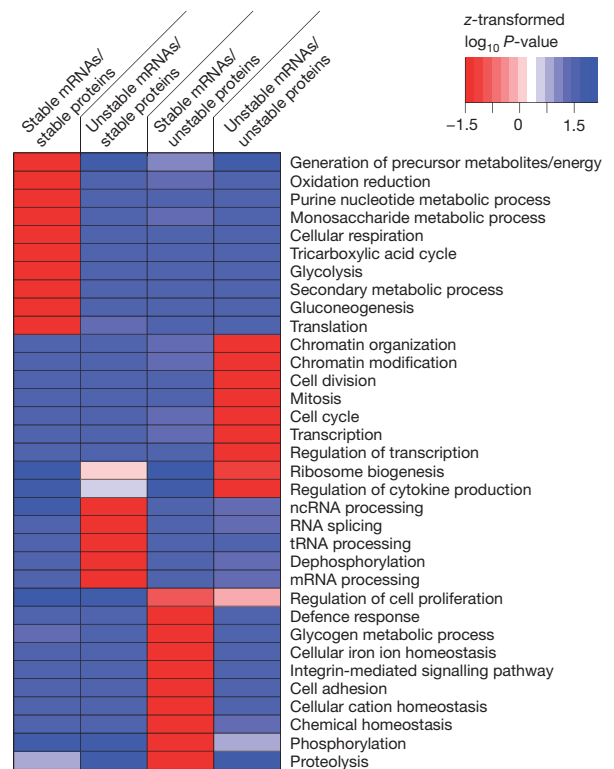
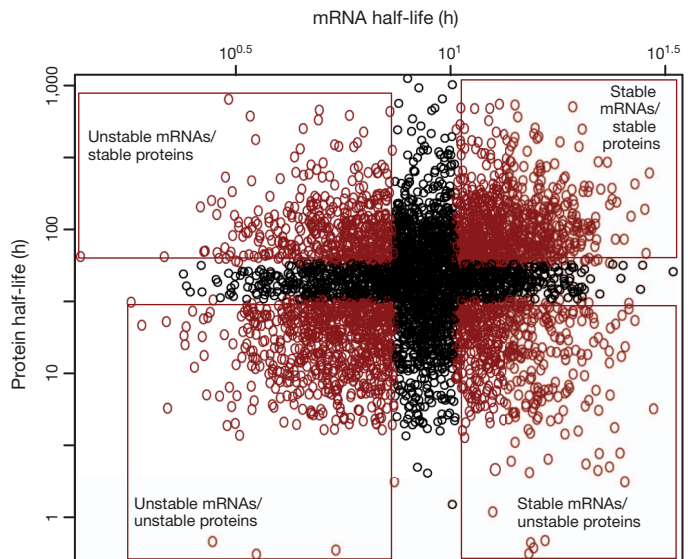


**Figure 5 | Functional characteristics of genes with different mRNA and protein half-lives.** Genes were grouped according to their combination of mRNA and protein half-lives and analysed for enriched gene ontology terms. A heat map of enrichment  $P$ -values reveals functional similarities of genes with similar combinations of half-lives.

(Fig. 4a). In addition, abundant proteins were significantly shorter (Supplementary Fig. 12b). Shuffling protein half-lives and lengths markedly increased theoretical energy consumption (Supplementary Fig. 12c). Collectively, these observations indicate that mammalian gene expression evolved under energy constraints.

The subset of genes with unstable mRNAs and proteins was strongly enriched in transcription factors, signalling genes, chromatin modifying enzymes and genes with cell-cycle-specific functions (Fig. 5). Because mRNAs and proteins are information carriers, their degradation can be interpreted as a built-in timer that controls the persistence of genetic

information<sup>34</sup>. It therefore makes intuitive sense that many regulatory genes have short mRNA and protein half-lives. However, it must be stressed that population-level data cannot provide information about individual cells or molecules.

The group of genes with stable proteins but unstable mRNAs was strongly enriched in terms related to processing of mRNAs, tRNAs and non-coding RNAs. Hence, many mammalian RNA-binding proteins are stable whereas their encoding transcripts are short lived, as also found in yeast<sup>35</sup>. Because many RNA-binding proteins bind their own message<sup>36</sup>, this observation is indicative of a post-transcriptional negative feedback loop for RNA-binding proteins. Consistently, we found that unstable mRNAs are enriched for binding motifs of RNA-binding proteins (Supplementary Fig. 10).

Finally, the subset of genes with stable mRNAs and unstable proteins was rich in extracellular proteins. This is expected, as secreted proteins have a short cellular half-life. Additionally, this group contains proteins involved in cellular homeostasis, defence response and proteolysis. This set contains two ferritin proteins that are rapidly upregulated in response to iron<sup>37</sup>. Ferritins are classic examples of translationally regulated genes. As translational regulation is not dependent on mRNA half-lives, genes with stable mRNAs can still be dynamically regulated as long as their protein half-lives are short. It is tempting to speculate that other homeostasis genes in this group are regulated at the level of translation.

## Discussion

Although gene expression is one of the most fundamental processes in biology it has never been quantified comprehensively. We provide the first analysis of mRNA and protein levels, half-lives, transcription rates and translation rate constants for thousands of genes. In the future, additional methods like sequencing of nascent transcripts and ribosome profiling may further refine this picture<sup>38,39</sup>.

We found that mRNA levels explain around 40% of the variability in protein levels. This fraction is higher than in previous studies on mammals<sup>3,4,23</sup>. We found that in mouse fibroblasts, translation efficiency is the single best predictor of protein levels. Hence, protein abundance seems to be predominantly regulated at the ribosome, highlighting the importance of translational control<sup>40,41</sup>. Whether this observation is valid in other cell types is not known. A recent study on embryonic stem cells revealed that changes in protein levels are not accompanied by changes in corresponding mRNAs<sup>42</sup>. It is also not clear how much translation rate constants change under different conditions. Our observation that the mouse model can to some degree predict levels of orthologous proteins in MCF7 cells suggests that translation efficiency is partially 'hard-coded' in the genome and is not subject to change.

Compared to translational control, protein stability seems to have a minor role in cellular protein abundance in our system. This is surprising as protein degradation is involved in the regulation of many cellular processes<sup>28–30</sup>. From the global perspective, the dominance of translational regulation makes sense given the high energy costs associated with protein synthesis. However, it should also be stressed that our data set represents average values derived from a population of dividing, non-synchronized cells. At the single cell level, the role of protein degradation for protein abundance may be higher. Similarly, protein degradation may be more important upon perturbation.

Gene expression may follow certain design principles for optimal evolutionary fitness. Intriguingly, we found that genes with certain combinations of mRNA and protein half-lives share common functions, indicating that they evolved under similar constraints. One of these constraints may be energy efficiency<sup>33</sup>. Consistently, we observed that the theoretical energy needed for gene expression is much lower than random. A second constraint may be the ability of genes to respond quickly to a stimulus. We find that many transcription factors and genes with cell-cycle-specific function have unstable mRNAs and proteins, predisposing them to rapid transcriptional and/or

translational regulation. In addition, genes with stable mRNAs but unstable proteins can be regulated quickly at the level of translation. These observations are consistent with the idea that many fast-responding genes have short protein and/or mRNA half-lives<sup>10,31,32,43</sup>. The global picture is that most mRNAs and especially proteins are stable unless genes need to respond quickly to a stimulus. Owing to the trade-off between dynamic regulation and energy efficiency, this may be an optimal design.

Our data provide a rich resource for the scientific community that can be mined in many ways that are beyond the scope of this study (see Supplementary Table 3 for the entire data set). For example, we provide by far the largest data set on protein copy numbers, which contains valuable information for modelling of cellular processes and stoichiometry of protein complexes<sup>22</sup>. Half-lives of proteins and mRNAs can be used to search for properties of unstable mRNAs or proteins, and we provide a first analysis of characteristic sequence features (Supplementary Figs 9 and 10). Genome-scale quantitative data on absolute mRNA and protein levels and half-lives will certainly help to understand the complex relationships between thousands of genes and their products in biological systems.

*Note added in proof:* While this paper was in revision, another paper<sup>44</sup> reported that changes in mRNA levels in dendritic cells are mainly determined by transcription rates. This result is consistent with our findings in fibroblasts. Notably, mRNA half-lives reported in ref. 44 are considerably shorter (see Supplementary Information for a brief discussion).

## METHODS SUMMARY

NIH3T3 cells grown in light (L) SILAC medium were simultaneously pulse-labelled with heavy (H) amino acids and 4-thiouridine (4sU). For proteome analysis, proteins were extracted, separated by SDS-polyacrylamide gel electrophoresis (PAGE), trypsin-digested and analysed by LC-MS/MS on high-resolution instruments (LTQ-Orbitrap XL and Velos, Thermo Fisher). Raw files were processed by MaxQuant (version 1.0.13.13) for peptide/protein identification and quantification. In total 3,588,163 fragment spectra led to 972,333 peptide identifications (84,676 unique peptide sequences) that were assigned to 6,445 unique proteins (false discovery rate of 1% at the peptide and protein level). Average absolute mass deviation was 0.29 parts per million (p.p.m.). Absolute protein amounts were calculated as the sum of all peptide peak intensities divided by the number of theoretically observable tryptic peptides (intensity based absolute quantification, or iBAQ). RNA was extracted and separated into newly synthesized and pre-existing fractions based on the incorporated 4sU. Total, pre-existing and newly synthesized RNA samples were processed according to an mRNA sequencing protocol (two rounds of oligo(dT) enrichment) and analysed on a Solexa GAIIIX sequencing platform (36 cycles). Reads were mapped to the mouse genome reference sequence (mm9, July 2007) using SOAP2 with a maximum of two mismatches allowed. Only uniquely mapped reads were retained. For more details on data acquisition, processing, analysis and modelling see Supplementary Methods.

Received 16 November 2010; accepted 1 April 2011.

1. Ben-Tabou de-Leon, S. & Davidson, E. H. Modeling the dynamics of transcriptional gene regulatory networks for animal development. *Dev. Biol.* **325**, 317–328 (2009).
2. Komili, S. & Silver, P. A. Coupling and coordination in gene expression processes: a systems biology view. *Nature Rev. Genet.* **9**, 38–48 (2008).
3. de Sousa Abreu, R., Penalva, L. O., Marcotte, E. M. & Vogel, C. Global signatures of protein and mRNA expression levels. *Mol. Biosyst.* **5**, 1512–1526 (2009).
4. Maier, T., Guell, M. & Serrano, L. Correlation of mRNA and protein in complex biological samples. *FEBS Lett.* **583**, 3966–3973 (2009).
5. Belle, A., Tanay, A., Bitincka, L., Shamir, R. & O'Shea, E. K. Quantification of protein half-lives in the budding yeast proteome. *Proc. Natl Acad. Sci. USA* **103**, 13004–13009 (2006).
6. Yang, E. *et al.* Decay rates of human mRNAs: correlation with functional characteristics and sequence attributes. *Genome Res.* **13**, 1863–1872 (2003).
7. Yen, H. C., Xu, Q., Chou, D. M., Zhao, Z. & Elledge, S. J. Global protein stability profiling in mammalian cells. *Science* **322**, 918–923 (2008).
8. Gouw, J. W., Krijgsveld, J. & Heck, A. J. Quantitative proteomics by metabolic labeling of model organisms. *Mol. Cell. Proteomics* **9**, 11–24 (2010).
9. Beynon, R. J. & Pratt, J. M. Metabolic labeling of proteins for proteomics. *Mol. Cell. Proteomics* **4**, 857–872 (2005).

10. Friedel, C. C., Dolken, L., Ruzsics, Z., Koszinowski, U. H. & Zimmer, R. Conserved principles of mammalian transcriptional regulation revealed by RNA half-life. *Nucleic Acids Res.* **37**, e115 (2009).
11. Mann, M. Functional and quantitative proteomics using SILAC. *Nature Rev. Mol. Cell Biol.* **7**, 952–958 (2006).
12. Doherty, M. K., Hammond, D. E., Clague, M. J., Gaskell, S. J. & Beynon, R. J. Turnover of the human proteome: determination of protein intracellular stability by dynamic SILAC. *J. Proteome Res.* **8**, 104–112 (2009).
13. Milner, E., Barnea, E., Beer, I. & Admon, A. The turnover kinetics of major histocompatibility complex peptides of human cancer cells. *Mol. Cell. Proteomics* **5**, 357–365 (2006).
14. Lam, Y. W., Lamond, A. I., Mann, M. & Andersen, J. S. Analysis of nucleolar protein dynamics reveals the nuclear degradation of ribosomal proteins. *Curr. Biol.* **17**, 749–760 (2007).
15. Schwanhäusser, B., Gossen, M., Dittmar, G. & Selbach, M. Global analysis of cellular protein translation by pulsed SILAC. *Proteomics* **9**, 205–209 (2009).
16. Selbach, M. *et al.* Widespread changes in protein synthesis induced by microRNAs. *Nature* **455**, 58–63 (2008).
17. Cox, J. & Mann, M. MaxQuant enables high peptide identification rates, individualized p.p.b.-range mass accuracies and proteome-wide protein quantification. *Nature Biotechnol.* **26**, 1367–1372 (2008).
18. Price, J. C., Guan, S., Burlingame, A., Prusiner, S. B. & Ghaemmaghami, S. Analysis of proteome dynamics in the mouse brain. *Proc. Natl Acad. Sci. USA* **107**, 14508–14513 (2010).
19. Wu, C. C., MacCoss, M. J., Howell, K. E., Matthews, D. E. & Yates, J. R. III. Metabolic labeling of mammalian organisms with stable isotopes for quantitative proteomic analysis. *Anal. Chem.* **76**, 4951–4959 (2004).
20. Mortazavi, A., Williams, B. A., McCue, K., Schaeffer, L. & Wold, B. Mapping and quantifying mammalian transcriptomes by RNA-Seq. *Nature Methods* **5**, 621–628 (2008).
21. Lu, P., Vogel, C., Wang, R., Yao, X. & Marcotte, E. M. Absolute protein expression profiling estimates the relative contributions of transcriptional and translational regulation. *Nature Biotechnol.* **25**, 117–124 (2007).
22. Malmström, J. *et al.* Proteome-wide cellular protein concentrations of the human pathogen *Leptospira interrogans*. *Nature* **460**, 762–765 (2009).
23. Vogel, C. *et al.* Sequence signatures and mRNA concentration can explain two-thirds of protein abundance variation in a human cell line. *Mol. Syst. Biol.* **6**, 400 (2010).
24. Geiss, G. K. *et al.* Direct multiplexed measurement of gene expression with color-coded probe pairs. *Nature Biotechnol.* **26**, 317–325 (2008).
25. Darzacq, X. *et al.* In vivo dynamics of RNA polymerase II transcription. *Nature Struct. Mol. Biol.* **14**, 796–806 (2007).
26. Arava, Y., Boas, F. E., Brown, P. O. & Herschlag, D. Dissecting eukaryotic translation and its control by ribosome density mapping. *Nucleic Acids Res.* **33**, 2421–2432 (2005).
27. Wu, G., Nie, L. & Zhang, W. Integrative analyses of posttranscriptional regulation in the yeast *Saccharomyces cerevisiae* using transcriptomic and proteomic data. *Curr. Microbiol.* **57**, 18–22 (2008).
28. Kirkpatrick, D. S., Denison, C. & Gygi, S. P. Weighing in on ubiquitin: the expanding role of mass-spectrometry-based proteomics. *Nature Cell Biol.* **7**, 750–757 (2005).
29. Hershko, A. & Ciechanover, A. The ubiquitin system. *Annu. Rev. Biochem.* **67**, 425–479 (1998).
30. King, R. W., Deshaies, R. J., Peters, J. M. & Kirschner, M. W. How proteolysis drives the cell cycle. *Science* **274**, 1652–1659 (1996).
31. Hao, S. & Baltimore, D. The stability of mRNA influences the temporal order of the induction of genes encoding inflammatory molecules. *Nature Immunol.* **10**, 281–288 (2009).
32. Legewie, S., Herzel, H., Westerhoff, H. V. & Bluthgen, N. Recurrent design patterns in the feedback regulation of the mammalian signalling network. *Mol. Syst. Biol.* **4**, 190 (2008).
33. Wagner, A. Energy constraints on the evolution of gene expression. *Mol. Biol. Evol.* **22**, 1365–1374 (2005).
34. Pedraza, J. M. & Paulsson, J. Effects of molecular memory and bursting on fluctuations in gene expression. *Science* **319**, 339–343 (2008).
35. Mittal, N., Roy, N., Babu, M. M. & Janga, S. C. Dissecting the expression dynamics of RNA-binding proteins in posttranscriptional regulatory networks. *Proc. Natl Acad. Sci. USA* **106**, 20300–20305 (2009).
36. Hogan, D. J., Riordan, D. P., Gerber, A. P., Herschlag, D. & Brown, P. O. Diverse RNA-binding proteins interact with functionally related sets of RNAs, suggesting an extensive regulatory system. *PLoS Biol.* **6**, e255 (2008).
37. Hentze, M. W., Muckenthaler, M. U. & Andrews, N. C. Balancing acts: molecular control of mammalian iron metabolism. *Cell* **117**, 285–297 (2004).
38. Ingolia, N. T., Ghaemmaghami, S., Newman, J. R. & Weissman, J. S. Genome-wide analysis *in vivo* of translation with nucleotide resolution using ribosome profiling. *Science* **324**, 218–223 (2009).
39. Churchman, L. S. & Weissman, J. S. Nascent transcript sequencing visualizes transcription at nucleotide resolution. *Nature* **469**, 368–373 (2011).
40. Gebauer, F. & Hentze, M. W. Molecular mechanisms of translational control. *Nature Rev. Mol. Cell Biol.* **5**, 827–835 (2004).
41. Sonenberg, N. & Hinnebusch, A. G. Regulation of translation initiation in eukaryotes: mechanisms and biological targets. *Cell* **136**, 731–745 (2009).
42. Lu, R. *et al.* Systems-level dynamic analyses of fate change in murine embryonic stem cells. *Nature* **462**, 358–362 (2009).
43. Rosenfeld, N., Elowitz, M. B. & Alon, U. Negative autoregulation speeds the response times of transcription networks. *J. Mol. Biol.* **323**, 785–793 (2002).
44. Rabani, M. *et al.* Metabolic labeling of RNA uncovers principles of RNA production and degradation dynamics in mammalian cells. *Nature Biotechnol.* doi:10.1038/nbt.1861 (24 April 2011).

**Supplementary Information** is linked to the online version of the paper at [www.nature.com/nature](http://www.nature.com/nature).

**Acknowledgements** We thank N. Rajewsky and L. Dölken for fruitful discussions and C. Sommer for technical assistance. M.S. and W.C. are supported by the Helmholtz Association, the German Ministry of Education and Research (BMBF) and the Senate of Berlin by funds aimed at establishing the Berlin Institute of Medical Systems Biology (BIMSB) (grant number 315362A). J.W. is supported by the ForSys-programme of the German Ministry of Education and Research (grant number 315289); D.B. by the Helmholtz Alliance on Systems Biology/MSBN; and N.L. by the China Scholarship Council CSC.

**Author Contributions** M.S. conceived, designed and supervised the experiments. B.S. performed wet-lab experiments, mass spectrometry and proteomic data analysis. D.B. and J.W. developed and employed the mathematical model. N.L. performed RNA-seq experiments. W.C. designed and supervised RNA-seq experiments. B.S., D.B., J.S., W.C. and M.S. analysed genome-wide data. G.D. helped in cycloheximide chase experiments and data analysis. B.S., D.B., J.S., J.W., W.C. and M.S. interpreted the data. M.S. wrote the manuscript.

**Author Information** Sequences have been deposited in the Sequence Read Archive under accession code SRA030871. Reprints and permissions information is available at [www.nature.com/reprints](http://www.nature.com/reprints). The authors declare no competing financial interests. Readers are welcome to comment on the online version of this article at [www.nature.com/nature](http://www.nature.com/nature). Correspondence and requests for materials should be addressed to J.W. ([jana.wolf@mdc-berlin.de](mailto:jana.wolf@mdc-berlin.de), for mathematical modelling), W.C. ([wei.chen@mdc-berlin.de](mailto:wei.chen@mdc-berlin.de), for transcriptomics) or M.S. ([matthias.selbach@mdc-berlin.de](mailto:matthias.selbach@mdc-berlin.de), for proteomics).



## CORRIGENDUM

doi:10.1038/nature11848

## Corrigendum: Global quantification of mammalian gene expression control

Björn Schwanhäusser, Dorothea Busse, Na Li, Gunnar Dittmar, Johannes Schuchhardt, Jana Wolf, Wei Chen & Matthias Selbach

*Nature* **473**, 337–342 (2011); doi:10.1038/nature10098

Mark Biggin of the Lawrence Berkeley National Laboratory contacted us, noting that our mass-spectrometry-based protein copy number estimates are lower than several literature-based values. We therefore re-analysed the scripts used for data processing, and found a scaling error that occurred during the conversion of normalized protein intensity values into absolute copy number estimates. As described in the original Article, slope and offset for scaling were calculated by linear regression based on an in-solution digest with spiked-in

proteins of known concentrations. We erroneously used the slope and the offset from an unrelated experiment to scale protein levels, resulting in a systematic underestimation of protein levels and derived translation rate constants. We apologize for this error and any confusion it may have caused.

When the error was corrected, the median levels of detected proteins increased about threefold and the ratio of average protein to messenger RNA increased from 900 to 2,800. The median and apparent maximum translation rate constants increased from 40 to 140 and from 180 to 1,000 proteins per mRNA per hour, respectively. Consequently, the estimated maximum translation rate constant in sea urchin embryos at 15 °C (140 proteins per mRNA per hour) is lower than our corrected prediction for mouse fibroblasts (1,000 proteins per mRNA per hour). All our conclusions about global gene expression control (correlations between mRNA and protein levels and half-lives, predominant control of protein abundance at the level of translation, functional properties of genes with specific half-life

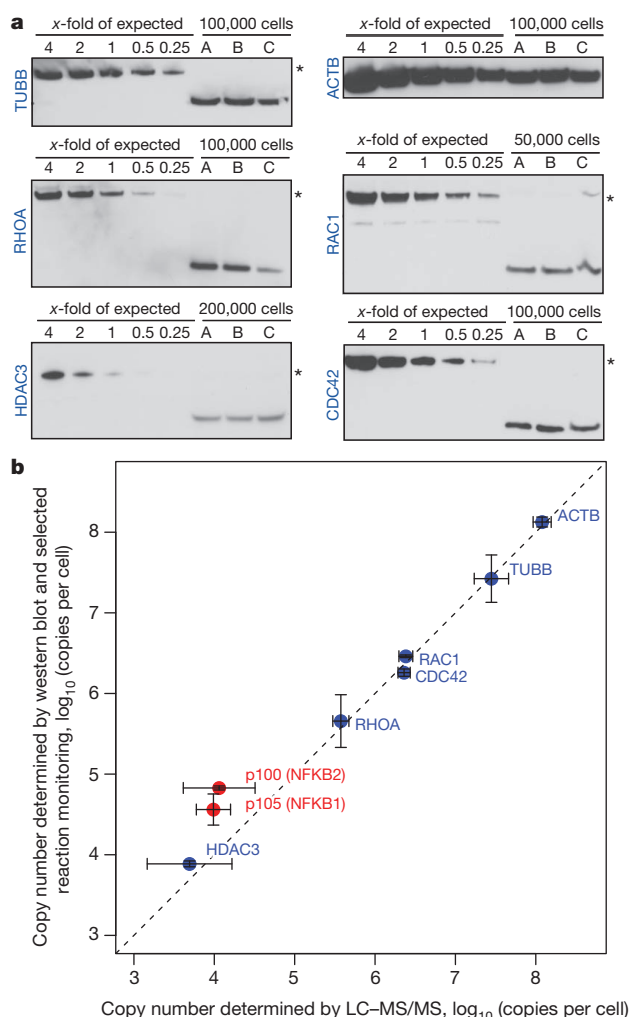


**Figure 1 | Comparison of LC-MS/MS-based protein copy number estimates in NIH3T3 cells with alternative methods.** **a**, Representative western blots of cellular proteins with dilution series of purified protein standards. Standards were diluted in a way that one-fold corresponds to the amount expected from the average of the LC-MS/MS-based estimates. The asterisks indicate the position of the GST-fusion proteins. **b**, Comparison of estimates based on western blots (blue,  $n \geq 3$ ) and selected reaction monitoring (red,  $n = 3$ ) with our LC-MS/MS data ( $n = 2$ ). Error bars show standard deviations.

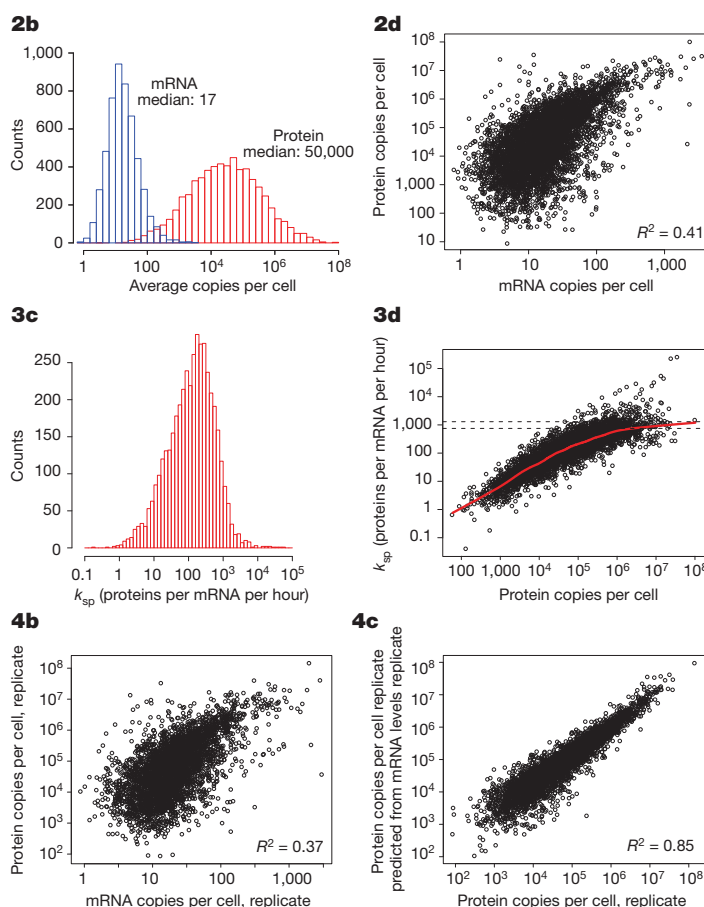


**Figure 2 | This figure shows the corrected panels for Figs 2b and d, 3c and d and 4b and c of the original Article.** We note that although the distribution of data in the original and corrected figures appears very similar, the axes are different.

combinations and so on) are unaffected. Figure 2 of this Corrigendum shows the corrected Figs 2b and d, 3c and d and 4b and c. Supplementary Figs 5a and b, 6d and f, 8f, 12a and b, and Supplementary Tables 1 and 3 of the original Article have been corrected. Protein copy numbers and translation rate constants in the text and figures in the HTML and PDF versions of the original Article have been corrected.

To further validate copy numbers in NIH3T3 cells we performed western blots with a dilution series of purified human proteins as standards (Fig. 1a of this Corrigendum). Briefly, cells were washed, harvested by trypsinization, counted independently by two persons, lysed in radioimmunoprecipitation assay buffer (containing 1% SDS) and separated by SDS–polyacrylamide gel electrophoresis (PAGE). As standards, defined amounts of human glutathione-*S*-transferase (GST)-tagged HDAC3, TUBB (Abnova), RHOA, RAC1 or CDC42 (purified in house and quantified spectrophotometrically) or purified ACTB (Biotrend) were diluted in SDS sample buffer containing 0.07 µg *Escherichia coli* lysate per microlitre to minimize protein loss during dilution. Antibodies against HDAC3 (2632), CDC42 (2466) and Rac1/2/3 (2467) were from Cell Signalling; the ACTB (A5441)

and TUBB (T8328) antibodies were from Sigma and the anti-RHOA antibody (SC-418) was from Santa Cruz. Protein abundance in NIH3T3 cells was estimated densitometrically, based on the dilution series as a standard curve (Scion Image). We also used selected reaction monitoring to quantify two additional proteins (p100 and p105). To this end, cells were lysed (6 M urea, 2 M thiourea) and lysates mixed with synthetic-stable-isotope-labelled proteotypic peptides (SpikeTides, JPT Peptide Technologies). Samples were digested and analysed on a Q-Trap 5500 system (AB Sciex) in three technical replicates monitoring three transitions per peptide. Quantification was performed using Multiquant 1.2 (AB Sciex) based on the two most intense transitions. Overall, copy number estimates of the eight proteins obtained by alternative approaches correlated well with our data derived from liquid chromatography and tandem mass spectrometry (LC-MS/MS) (Fig. 1b of this Corrigendum), even though the two measurements based on selected reaction monitoring lie above the diagonal. The data are in good agreement with the expected precision and reproducibility of our large-scale absolute protein quantification approach (see Supplementary Figs 6d and 8b of the original Article).